Convection in Arc Weld Pools

Electromagnetic and surface tension forces are shown to dominate flow behavior, in some cases producing double circulation loops in the weld pool

BY G. M. OREPER, T. W. EAGAR, AND J. SZEKELY

ABSTRACT. A mathematical model has been developed to account for convection and temperature distributions in stationary arc weld pools driven by buoyancy, electromagnetic and surface tension forces. It is shown that the electromagnetic and surface tension forces dominate the flow behavior. In some cases, these forces produce double circulation loops, which are indirectly confirmed by experimental measurements of segregation in the weld pool. It is also shown that the surface tension driven flows are very effective in dissipating the incident energy flux on the pool surface which, in turn, reduces the vaporization from the weld pool.

Introduction

The quantitative understanding of convection and heat flow in weld pools is of considerable practical interest because convective heat flow will affect the weld pool geometry, fume formation, and grain structure in the resulting weld bead. It has been appreciated in a qualitative sense that significant fluid motion may occur in weld pools encountered in arc welding. However, up to the present time, the quantitative treatment of these phenomena has been extremely limited. Indeed the previous work may be classified into the following main groupings:

1. In the vast majority of heat flow analyses, no allowance has been made for convective heat flow in the melt, or at the most an effective thermal conductivity has been postulated to provide a qualitative representation of the enhanced heat transfer (Ref. 1).

2. In recent work by Atthey (Ref. 2), a hemispherical weld pool shape was postulated and fluid flow calculations were made for a highly idealized, isothermal system where electromagnetic forces constituted the sole driving force.

3. The quasi steady state development of weld pools as driven by a combination of buoyancy and electromagnetic forces was considered by Oreper and Szekely (Ref. 3) who found that, under certain conditions, convective motion (particularly due to electromagnetic forces) did play an important role in modifying the weld pool shape.

In addition to these limited analyses, there is extensive literature dealing with practical observations concerning weld pool behavior. Up to the present, however, it has been rather difficult to develop a meaningful relationship between theoretical models and experimental observations. One possible reason for this dichotomy is the great complexity of these systems and the possible interactive role played by a number of driving forces, which have to include surface tension, buoyancy and electromagnetic forces.

The purpose of this paper is to examine the behavior of a somewhat idealized stationary weld pool in order to define the principal conditions that govern heat transfer and convection. The actual input conditions for the model will be so chosen as to reflect actual operating practice. Thus, the conclusions that may be drawn from the computed results should have practical relevance.

Formulation

Figure 1 shows a schematic sketch of an arc welding system. It is seen that a plasma arc, which acts as a distributed source of heat and electric current, impinges onto a molten metal pool; this provides an incident flux of current and thermal energy at the free surface of the weld pool. The actual shape of the weld pool and the spatial distribution of the current and of the heat flux may be specified for a given application. Motion in the weld pool is due to three distinct forces:

1. The divergent current path in the melt will generate a magnetic field, the interaction of which with the current will give rise to electromagnetic, or Lorentz, forces.

2. The temperature gradients within the melt will give rise to buoyancy forces.

3. The temperature gradients at the free surface and possibly the spatial distribution of surface active components in the melt will give rise to surface tension driven flows.

In this paper, the problem is formulated in the following manner:

1. We consider laminar flow, which is thought to be reasonable in view of the small size of the system.

2. We postulate a given weld pool shape, taken from a distributed heat source theory employing pure conduction and in general agreement with practical experience (Ref. 4).

3. We postulate the spatial distribution of the electric current falling on the weld

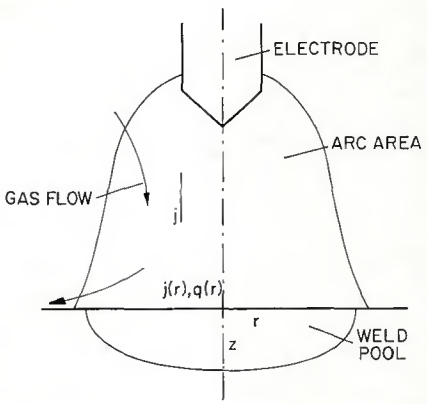

Fig. 1—Schematic of welding arc showing relative size of weld pool, electrode and arc

G. M. OREPER, (Research Assoc.), T. W. EAGAR (Assoc. Prof.—Materials Engineering), and J. SZEKELY (Prof.—Materials Engineering) are with the Department of Materials Science and Engineering, M.I.T., Cambridge, Mass.

pool, taken from experimental measurements on water cooled copper anodes (Ref. 5).

4. We postulate the spatial distribution of the heat flux falling on the weld pool; here again these data are taken from actual measurements on water cooled copper anodes (Ref. 5).

Then the problem may be stated by the following equations (see Table 1 for symbols and their definitions):

(a) The equation of continuity

$$\nabla \cdot \underset{\sim}{V} = 0 \quad (1)$$

(b) The equation of motion

$$\rho(\underset{\sim}{V} \cdot \nabla)\underset{\sim}{V} = -\underset{\sim}{\Delta} P + \mu\nabla^2\underset{\sim}{V} + \underset{\sim}{F}_b \quad (2)$$

where $\underset{\sim}{F}_b = \underset{\sim}{J} \times \underset{\sim}{B} - \rho g\beta(T - T_o)$ the body force incorporates both the electromagnetic and the buoyancy forces (Ref. 3).

The former may be obtained through the solution of Maxwell's equations. On the other hand, the latter is obtained through the simultaneous solution of the convective heat flow equation, which takes the following form:

$$\rho C_p(\underset{\sim}{V} \cdot \nabla)T = \kappa_m\nabla^2 T \quad (3)$$

The boundary conditions employed for the solution of these equations will need to express the physical facts of symmetry about the centerline and that the velocities are zero at the solid surfaces. In addition, there is the following:

$$T = T_{me},\ V = 0 \text{ at the interface} \quad (4)$$

$$q(r) = \frac{Q}{2\pi\sigma_q^2} \exp\left(-\frac{r^2}{2\sigma_q^2}\right)$$

specifying the heat flux at $z = 0$ (5)

$$j(r) = \frac{I}{2\pi\sigma j^2} \exp\left(-\frac{r^2}{2\sigma j^2}\right)$$

specifying the current at $z = 0$ (6)

and

$$\mu\frac{\partial V_r}{\partial z} = -\frac{\partial\gamma}{\partial T}\frac{\partial T}{\partial r} \quad (7)$$

Table 1—Symbols and Definitions[a]

C_p	-specific heat, 753 $\frac{J}{Kg \cdot K}$
D	-depth of a molten pool, mm
$\underset{\sim}{F}_b$	-body forces vector
$\underset{\sim}{I}$	-total electric current from the arc, A
j_s	-electric current density at the surface, A/m^2
κ_m	-thermal conductivity, 40.0 $\frac{w}{mK}$
P	-pressure, N/m^2
Q	-total heat input from the arc, $\frac{J}{S}$
r	-radial coordinate
W	-width of the molten pool, mm
T	-temperature, K
T_o	-reference temperature, K
T_{me}	-melting temperature, K
$\underset{\sim}{V}$	-velocity vector
V_r	-velocity component in r direction, m/s
z	-axial coordinate, m
β	-coefficient of volume expansion, $10^{-4}K^{-1}$
γ	-surface tension, N/m
μ	-viscosity, 0.006 $\frac{Kg}{mS}$
ρ	-density 7.2 · 10^3 $\frac{Kg}{m^3}$
σ_j	-current distribution parameter defined by equation (5)
σ_q	-heat distribution parameter defined by equation (6)
$Ma = \left\lvert\frac{\partial\gamma}{\partial T}\right\rvert Qp C_p/\kappa_m{}^2\mu$	Marangoni number

(a) Numerical values given are typical of carbon steel.

Equation (7) expresses the fact that the rate at which shear is being transferred into the fluid must be equal to the surface tension gradient, as caused by the temperature dependence of the interfacial tension. If surface tension effects had been ignored, the right hand side of equation (7) would have been zero.

Two additional stipulations were made in order to complete the statement of the boundary conditions. One of these was that the temperature of the free surface of the weld pool was bounded by an upper value corresponding to the temperature when the heat loss by vaporization equals the incident heat flux. As a practical matter, this value is at least 500 K (*i.e.*, 500°C or 900°F) below the boiling temperature (Ref. 8).

Finally, a planar free surface was assumed that was thought to be reasonable for values of current less than 250 amperes. The momentum transfer from the plasma arc was neglected as well as radiation loss (Ref. 9). It has been noted by others that the energy lost by radiation is small (Ref. 10), while evaporative cooling imposes an upper temperature limit on the surface of the weld pool (Ref. 8).

Upon considering cylindrical symmetry, the governing equations were put in a finite difference form, using an 8 X 10 unevenly spaced grid and were then solved numerically. The typical computer time requirements were about 0.5 minute CPU time of MIT's IBM 370 digital computer.

Computed Results

A selection of the computed results based on the thermal properties of carbon steel is presented below. The selection illustrates the effect of the principal input variables as summarized in Table 2. A total of eight runs are discussed and, as seen in Table 2, the principal variables were as follows:

- Q represents total heat input and, I, the total current passing through the system, the values of which were selected to correspond to both typical GTA welding conditions and the experimental measurements (Ref. 5).
- σ_q and σj represent the heat flux distribution parameters as previously defined in equations (5) and (6); these will

Table 2—Input Parameters Used For Calculations and Calculated Velocity Maxima

Run number	Total heat Q, J/s	Heat distribution parameter σ_q, mm	Total current I, A	Current distribution parameter σ_j, mm	Coefficient of surface tension, $\frac{\partial\gamma}{\partial T}$ dyn · cm^{-1} · K^{-1}	Marangoni numbers $Ma/10^5$	Weld width W, mm	Weld depth D, mm	Maximum velocity V, max mm/s
1	1143	1.6	100	1.3	−.49	4.22	4.0	1.8	838
2	1143	2.4	100	1.9	−.49	4.22	4.2	1.1	600
3	1524	1.6	190	1.6	−.49	4.22	4.1	2.4	950
4	1524	2.4	190	2.1	−.49	4.22	5.1	1.8	642
5	1524	1.6	190	1.4	−.25	2.15	4.1	2.4	665
6	1524	1.6	190	1.4	.25	2.15	4.1	2.4	−777[a]
7	1524	1.6	190	1.4	.49	4.22	4.1	2.4	−1259[a]
8	1524	1.6	190	1.4	.0	.0	4.1	2.4	−91[a]
9	1143	1.6	100	1.3	.0	.0	4.0	1.8	−45[a]
10	1143	2.4	100	1.9	.0	.0	4.2	1.1	−12[a]
11	1524	2.4	190	2.1	.0	.0	5.1	1.8	−48[a]

(a) Negative values of velocity represent radially inward flow.

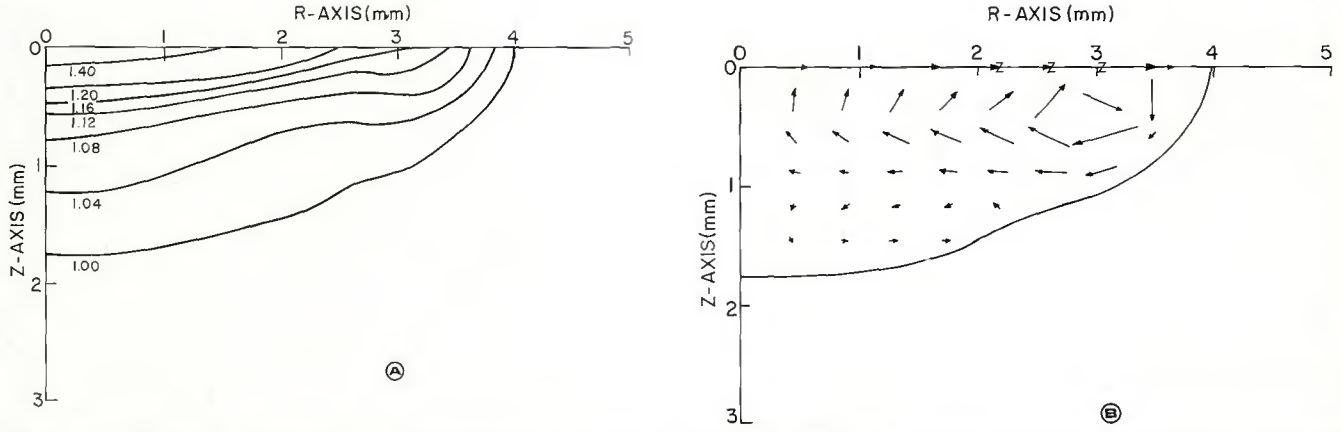

Fig. 2—Results for run no. 1 of Table 2: A—computed isotherms expressed as a fraction of the absolute melting temperature for a stationary weld with the parameters of run no. 1; this represents a sharply focused 100 A arc. B—computed velocity map

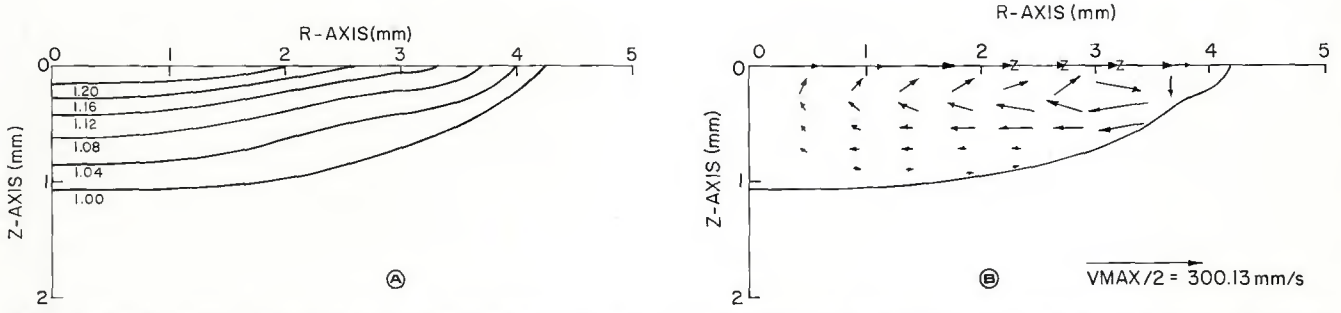

Fig. 3—Results for run no. 2 of Table 2: A—computed isotherms for run no. 2, representing a broadly focused 100 A arc. B—computed velocity map

determine whether the heat flux and the incident current are sharply focused or broadly distributed.

- $\frac{\partial \gamma}{\partial T}$ represents the temperature

dependence of the surface tension and the range examined corresponds to the property values of practical systems. The actual numerical values may be either positive or negative depending on the role played by impurities (Ref. 6).

- W and D represent the width and the depth of the weld pool which were specified *a priori* using the experimental values of Tsai (Ref. 5) and which were represented by the following relationship:

$$z = D\left[1 - \frac{r}{\sqrt{w}}\right]$$

Figures 2-5 show the computed results corresponding to the first four entries in Table 2.

Figures 2 and 3 represent current inputs of 100 A but corresponding to sharply focused heat and current inputs and broadly distributed heat and current inputs, respectively. It is seen that the velocity field is dominated by surface tension effects in both cases; however, the absolute value of the maximum velocity is significantly higher due to the sharply focused heat input. This represents behavior that is clearly consistent with physical reasoning, because the sharply focused heat input will give rise to steeper temperature gradients and hence to steeper surface tension gradients at the free surface.

A double loop circulation pattern is barely discernible but can be more readily seen in Figs. 4 and 5. Further, it is seen that the sharply focused heat input will produce a deeper weld pool; however, this is an input into the model calculations rather than a result of the computation.

It should be noted that, for the conditions depicted in Figs. 2 and 3, the surface temperature was well below the threshold level at which significant vaporization would occur. Thus, it was not necessary to invoke the limiting boundary condition specifying a maximum allowable temper-

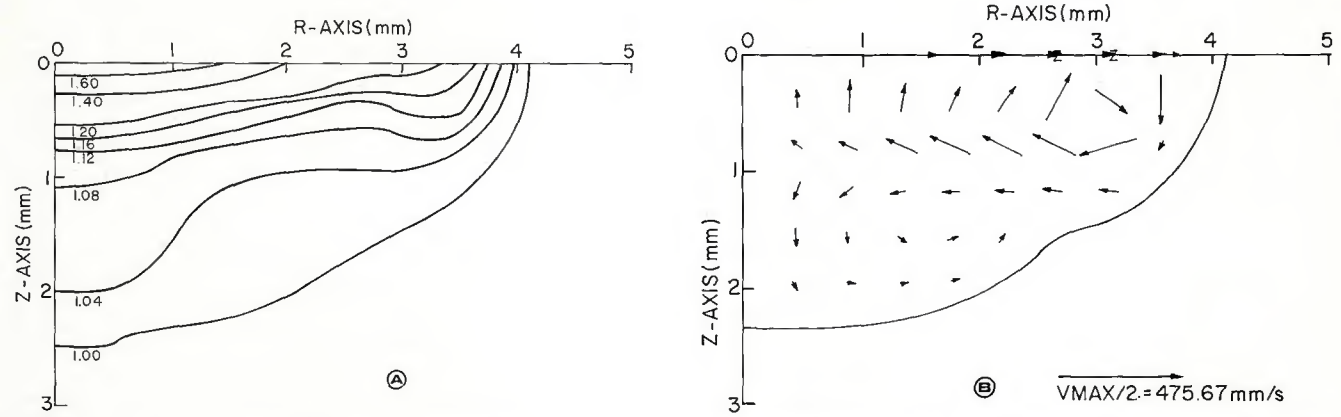

Fig. 4—Results for run no. 3 of Table 2: A—computed isotherms for run no. 3 representing a sharply focused 190 A arc. B—computed velocity map

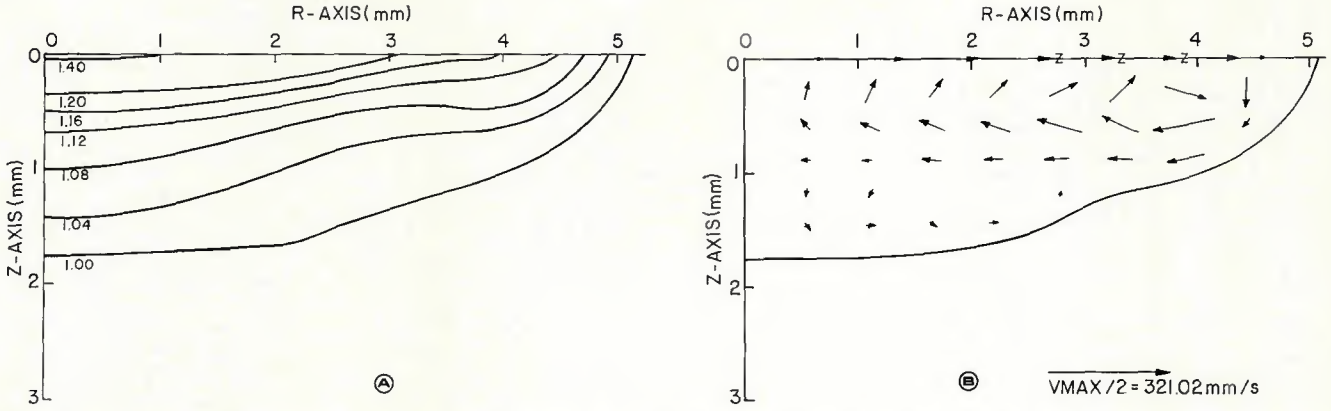

Fig. 5—Results for run no. 4 of Table 2: A—computed isotherms for run no. 4 representing a broadly focused 190 A arc. B—computed velocity map

ature.

Figures 4 and 5 show the computed results corresponding to entries 3 and 4 in Table 2. These involve a higher current and heat input and again correspond to a sharply focused and a broad distribution, respectively.

Inspection of Figs. 4 and 5 shows a significantly larger weld pool and also somewhat higher velocities. It is also seen that the absolute values of the maximum velocity are significantly higher due to the sharply focused heat input which parallels the behavior exhibited in Figs. 2 and 3.

Inspection of Figs. 4A and 5A shows that, in this case, the critical temperature was being approached in the central region of the weld pool due to the significantly higher heat input. Furthermore, examination of Fig. 4B clearly indicates the double loop circulation pattern. The flow field in the vicinity of the free surface is dominated by surface tension effects, while the counter-clockwise circulation pattern discernible in the lower part of the pool is due to electromagnetic forces. This is an interesting trend in that higher currents will produce deeper weld pools and will, at the same time, give rise to stronger electromagnetic forces. It follows that the relative importance of surface tension and electromagnetic forces depends quite critically on the precise nature of the operating conditions.

Figure 6 depicts results corresponding to the input data of entry 8 in Table 2. The input data are identical to entry 3 except for the fact that the surface tension forces were considered negligible.

Upon comparing Figs. 4 and 6, the following may be noted:

1. There is a significant difference in both the overall circulation pattern and in the absolute magnitude of the melt velocities. The circulation is driven entirely by electromagnetic forces, and the absolute value of the maximum velocity is less than 20% of that previously found.

2. While the postulated shape of the weld pool is the same (this was necessarily the case because of the *a priori* imposed conditions), there are significant differences in the maps of the isotherms. In the absence of surface tension driven flows, the maximum surface temperature approaches the limiting temperature over a much larger portion of the domain, and the local gradients are steeper. It is apparent on inspection of Figs. 4A and 6A that the postulated weld pool shape is much more consistent with the isotherms found in Fig. 4A than for Fig. 6A. The result of the additional calculations are presented in Table 2.

Runs 3 and 5-8 in Table 2 also summarize the role played by the temperature dependence of the surface tension in determining the value and the sign of the maximum velocity in the weld pool. It is seen that the numerical value of $\frac{\partial \gamma}{\partial T}$ or of the Marangoni number plays an important role in determining both the sign and the absolute value of the maximum velocity. This seems reasonable on physical grounds because when surface tension forces are present, they are likely to be the dominant factor in determining the maximum melt velocity which will be at the free surface.

When surface tension forces are due to temperature gradients only, these will promote a clockwise circulation pattern. Positive values of $\frac{\partial \gamma}{\partial T}$ may occur under

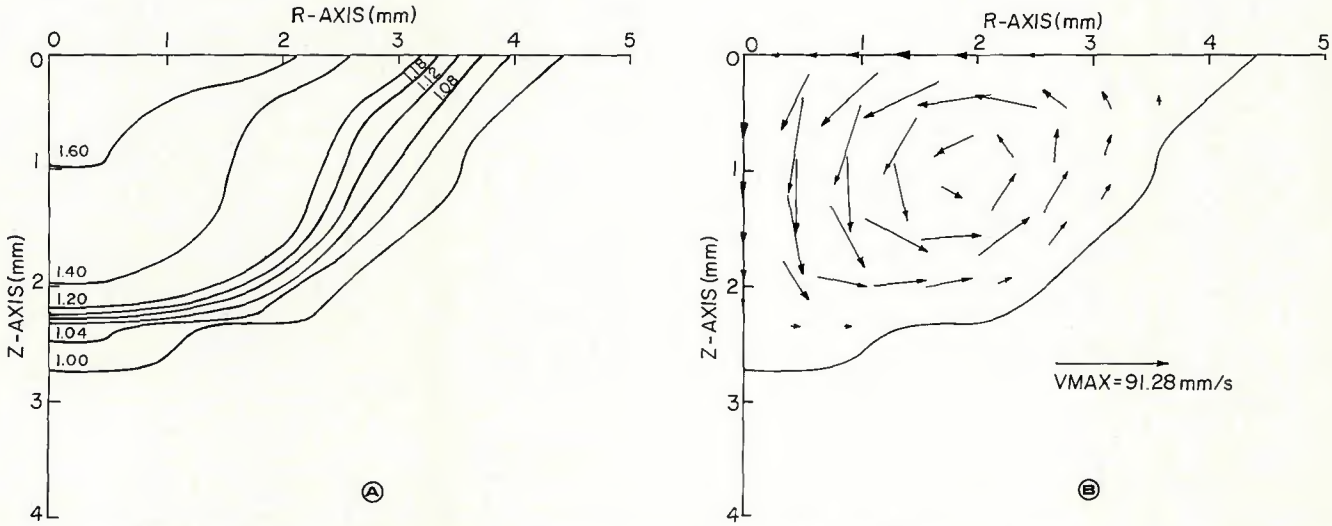

Fig. 6—Results for run no. 8 of Table 2: A—computed isotherms for run no. 8 representing a sharply focused 190 A arc without surface tension driven flow taken into account. B—computed velocity map

certain circumstances due to the role played by the presence of impurities. In any case, careful attention must be paid to surface tension effects, because these may dominate the flow field.

Runs 8-11 in Table 2 also show the role played by the weld current and its distribution in determining the maximum melt velocities in the absence of surface tension effects. It is seen that the absolute values of the velocity are much smaller (say, by a factor of 5–10) when surface tension effects are neglected and, as was previously shown, the Lorentz force dominated flow will produce a counterclockwise circulation pattern.

Table 2 also indicates that the maximum velocity produced by the electromagnetically driven flow is markedly dependent on both the system geometry and on the current distribution. A high, strongly focused current will produce the highest maximum velocity, because under these conditions the divergence of the current is the greatest. Furthermore, the deeper pool will provide a smaller surface to volume ratio.

Discussion

In this paper a mathematical representation has been developed for heat transfer and convection in weld pools. Attention is focused on the role played by thermal natural convection, electromagnetic forces and surface tension forces.

The model is approximate to the extent that steady state conditions were considered and that the weld pool shape was specified *a priori*. Additionally, however, the results of this work are thought to provide a greatly improved insight into the behavior of weld pools compared to what has been available up to the present. The actual input parameters (including the shape and size of the weld pool) were selected to correspond both to the range of conditions encountered in practice and to the experimental studies in order to allow a direct comparison of the model with measurements.

The practical conditions examined included the absolute magnitude of the energy input, the current and the heat flux distribution, and the role of surface tension forces.

The principal findings may be summarized as follows:

1. This is the first time that detailed velocity and temperature fields have been generated for GTA weld pools for realistic input conditions. This information is a key input for the proper study of solidification phenomena, the morphology and segregation phenomena in particular.

2. The calculations in which allowance has been made for surface tension driven flows, predicted quite high surface velocities – in the region of 60–120 cm/s (762–1524 ft/min). These values are within the range of those reported by Heiple and Roper (Ref. 6). Had surface tension effects been neglected, these velocities would have been much smaller.

3. The double circulation loops depicted in some of the computed results, notably in Fig. 4B, which result from the combined effect of surface tension driven flows and electromagnetically driven flows, are consistent with experimental observations. In this regard, Fig. 7 shows a photograph of a GTA spot weld on stainless steel; its shape is clearly consistent with both the isotherms shown in Fig. 4A and the associated circulation pattern given in Fig. 4B.

Figure 8, taken from the work of Savage (Ref. 7), shows the existence of localized unmixed regions in a weld pool. This behavior is again fully consistent with a laminar double loop circulation which was exhibited by the computed results.

The surface tension driven flows were important regarding their dominance of the overall circulation pattern under certain circumstances; in addition the high surface velocities were found to play a key role in the effective dissipation of the energy flux impinging onto the surface. On comparing the temperature fields in Figs. 4A and 6A, this rapid surface flow is seen to be quite significant in reducing the size of the high temperature zone in the impact area. As a result of convective cooling of the surface, vaporization from the weld pool is substantially reduced.

The principal finding of the work regarding insight into the weld pool behavior may be summarized by stating that significant convection, which is driven by the combination of surface tension, electromagnetic and buoyancy forces, exists in weld pools. Surface tension forces appear to be dominant in many instances.

Convection plays an important role in defining heat transfer and the position of the isotherms within the melt. Convection may also have a very marked effect in determining the shape of the weld pool and the associated solidification phenomena, which in turn could be crucial in determining the integrity of the weld.

It is thought that this paper represents a significant step toward quantifying these effects. However, a great deal of further work will be required as is apparent from a critical review of the simplifying assumptions made in the development of the model.

The principal assumptions made in the model development were the following:

1. Steady state.
2. Laminar flow.
3. The weld pool shape was specified *a priori*.
4. The incident current and heat fluxes were specified *a priori*.

The assumption of steady state conditions was thought to be reasonable as a first approximation, especially as experimentally determined weld pool shapes and input conditions were utilized for corresponding conditions.

The assumption regarding laminar flow was thought to be reasonable in view of the relatively small size of the weld pools

Fig. 7 – Profile of a stationary weld made for 3 s at 235 A on Type 304 stainless steel plate; compare this actual profile with the shape of the computed isotherms shown in Fig. 4A

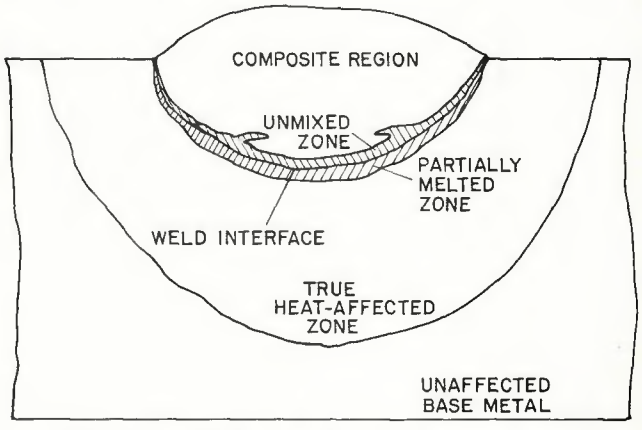

Fig. 8 – Mixing profile of high alloy Type 310 stainless steel on lower alloy Type 304 stainless steel base metal as measured by Savage et al. (Ref. 7). Note the protrusions of unmixed but fused base metal suggesting the presence of stagnation points in the velocity profile

considered. It is customary to use the Reynolds number $Re = \rho UL/\mu$ to determine whether the flow is laminar or turbulent, although the specific numerical value at which this transition occurs has to depend on the geometry. Here U is a characteristic velocity, L is a characteristic length. If one were to take U as the maximum velocity and L as the depth or the width of the weld pool, then one would obtain Reynolds numbers in the range of 2,000–3,000.

The maximum velocity obtained above is confined to a very small region in the vicinity of the free surface where significant turbulence damping may occur due to surface tension forces and the magnetic field. Furthermore, the mean velocity in the bulk is some ten times less than the maximum found near the surface. Thus, for the situation considered, the assumption of laminar flow seems reasonable. However, turbulence phenomena could well be important in weld pools of larger size and when higher currents are being used.

The *a priori* specification of the weld pool shape was necessary in the steady state calculations performed here; as noted earlier, this assumption may be justified by the fact that the experimentally determined weld pool shapes were used in the calculations. Furthermore, the computed isotherms were found to be consistent with the weld pool shapes when surface tension driven flows were taken into consideration (see Fig. 4A).

The assumption that the incident current and heat fluxes may be specified was necessary, because of the absence of information on the plasma regions at this stage. The actual distributions used were thought to be reasonable, because they were deduced from experimental measurements on water cooled copper anodes. It is realized, however, that there may be two-way interactions between the weld pool and the arc. The interactions would be due to vaporization of weld pool constituents that depends on the bath circulation and these might change the electrical properties of the arc and hence the heat flux distribution. Work is currently in progress to resolve some of these problems.

Conclusion

The model presented in this paper helps to confirm the work of Heiple and Roper (Ref. 6) which shows that surface tension driven flows dominate convection in the arc weld pool. As such, this model is much more correct than others which have neglected this factor. The velocities predicted by the model are in general agreement with experimentally measured values; however, the results show that small amounts of contaminants which alter the temperature dependence of surface tension can markedly influence both the magnitude and the direction of the flow as has been suggested by Heiple and Roper. This model will allow one to predict the shape and penetration of the weld pool under various process conditions and base metal compositions in at least a qualitative sense. An example of such a prediction has been given here.

In addition, the demonstration of stagnation points within the pool may be helpful in explaining the formation of "wagon track" slag inclusions and possibly other types of discontinuities which occur during welding.

Useful extensions of this work should account for flow in the presence of significant surface depression and in a travelling rather than a stationary mode. The good agreement of the present model with selected experimental results gives confidence that these more difficult models may provide a realistic description of convection in the more common arc welding situations. Such work is currently in progress.

Acknowledgment

The authors wish to express their appreciation for support of this work by the Office of Basic Energy Sciences, U.S. Department of Energy on Contract No. DE-AC02-78ER 94799.A0004.

References

1. Kou, S., Konevsky, T., and Fyfitch, S. 1982. Welding thin plates of aluminum alloys—a quantitative heat-flow analysis. *Welding Journal 61*(6):175-s to 181-s.

2. Atthey, D. R. 1980. A mathematical model for fluid flow in a weld pool at high currents. *J. Fluid. Mech.* 98:787-801.

3. Oreper, G. M., and Szekely, J. On electromagnetically and buoyancy driven flows in weld pools. Submitted to *J. Fluid Mech.*

4. Tsai, N.-S. and Eagar, T. W. 1983. Temperature fields produced by travelling distributed heat sources. Paper presented at the 64th Annual AWS Conference, April 24-29, Philadelphia, Pennsylvania.

5. Tsai, N.-S. 1983. *Heat Flow in Arc Welding.* Ph.D. thesis, Massachusetts Institute of Technology.

6. Heiple, C. R., and Roper, J. R. 1982. Mechanism for minor elements effect on GTA fusion zone geometry. *Welding Journal 61*(4):97-s to 102-s.

7. Savage, W. F., Baeslack III, W. A., and Lippold, J. C. 1979. Unmixed zone formation in austenitic stainless steel weldments. *Welding Journal 58*(6):168-s to 176-s.

8. Block-Bolten, A., and Eagar, T. W. 1982. Selective evaporation of metals from weld pools. *Trends in welding research in the United States, pp. 53-73.*Metals Park, Ohio: ASM.

9. Cobine, J. D., and Burger, E. E. 1955. Analysis of Electrode Phenomena in the High Current Arc, *J. Appl. Phys., 26*(7):895-900.